Chemical Engineering Journal 109 (2005) 89–96

Chemical Engineering Journal

www.elsevier.com/locate/cej

Intrinsic channel maldistribution in monolithic catalyst support structures

C. van Gulijk [a,*], M.J.G. Linders [a], T. Valdés-Solís [b,1], F. Kapteijn [b]

[a] *TNO Prins Maurits Laboratory, PO Box 45, 2280AA Rijswijk, The Netherlands*
[b] *Reactor and Catalysis Engineering, Delft University of Technology, Julianalaan 136, 2428BL Delft, The Netherlands*

Received 15 November 2004; received in revised form 22 March 2005; accepted 30 March 2005

Abstract

The paper introduces a straightforward method to measure intrinsic channel maldistribution in monolithic structures in gas–solid operation. The experimental procedure is non-destructive for the monolith and easy to perform but special care has to be taken to prevent leakage. The method is demonstrated for squared channel monoliths of 100 and 400 cells per square inch (cpsi). Variances in the production process of monoliths introduce an intrinsic channel maldistribution that can be described by a normal distribution. As a consequence, the assumption that a monolith is a bundle of equal channels is incorrect and may introduce significant errors in mathematical models that do not incorporate intrinsic channel maldistribution.

Keywords: Catalyst support; Monolith; Channel maldistribution

1. Introduction

Monolithic catalyst support structures have a special shape that gives them an advantage over conventional pellet catalyst supports. Monolithic catalyst supports are defined here as continuous unitary structured supports containing many narrow, parallel straight passages in a ceramic, metallic, carbon or plastic material. Fig. 1 shows square parallel channels in a cross-section of a cylindrical ceramic monolith. When compared to conventional packed bed reactors, the special shape of the monolith results in a low pressure drop, efficient catalyst usage, and presumably an easy scale-up. These advantages lead to the application of monoliths in many industrial processes. Single-phase flow applications include automotive exhaust after treatment [1–4]; selective catalytic reduction of NO_x [3–8]; adsorption of gases [9–11]; and selective oxidation (BASF). More recently, the opportunities in multiphase catalytic processes have been recognized, leading to increased research interest in this area. These processes include hydrogenation, oxidation and decomposition reactions [4,12]. The production of H_2O_2 [13] is an industrial application example. The hydrodynamic behavior of gases and liquids through the monolith is a key factor in understanding and prediction of monolithic catalyst performance. The hydrodynamic properties for single-phase flow are based on channel flow models [14]. Hydrodynamics in especially multi-phase flow is challenging and received much attention as well in the open literature [4,12,15–19].

The pressure drop of monoliths in practical applications is often governed by choosing cell densities, gas loads, and reactor sizes. Therefore, it is difficult to extract "characteristic" pressure drop for industrial processes from the literature. Some approximate figures include [4,11]: respiratory protection 10–100 Pa/m; automotive exhaust after treatment: up to 20,000 Pa/m with reactors of 15–30 cm; concurrent multiphase flow about 5000 Pa/m; automotive selective catalytic reduction of NO_x: up to 10,000 Pa/m with reactors between 30 and 50 cm; industrial selective catalytic reduction between 2000 and 10,000 Pa/m per stage of up to 1 m in length with up to a dozen of stages sequentially per reactor.

Flow-maldistribution of gases and liquids is a special hydrodynamic problem in monolithic catalysts. In theory, each

* Corresponding author. Tel.: +31 15 2843283; fax: +31 15 2843963.
E-mail address: gulijk@pml.tno.nl (C. van Gulijk).
[1] Present address: INCAR, Oviedo, Spain.

1385-8947/$ – see front matter © 2005 Elsevier B.V. All rights reserved.
doi:10.1016/j.cej.2005.03.013

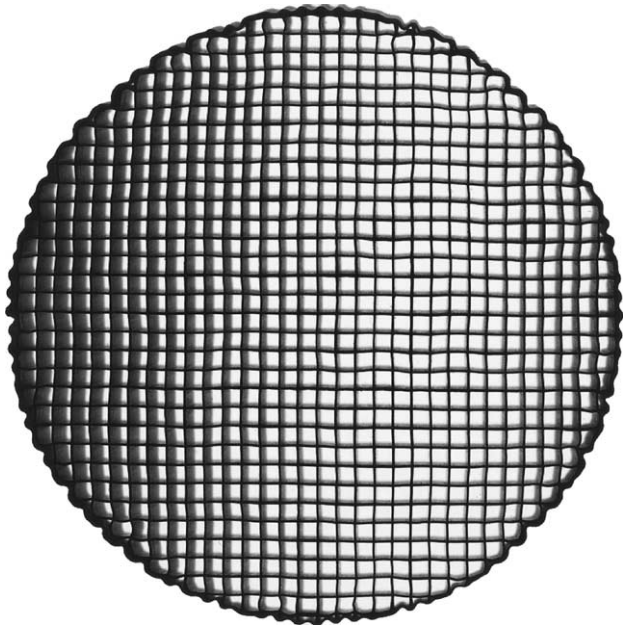

Fig. 1. Variances in monolith channels in a cross-section of a 400 cpsi carbon coated cordierite monolith.

channel in the monolith acts as a single plug-flow reactor. If the reactant flow through some channels is higher than in others the residence time of the reactants varies and with it, the concentration of products. This leads to inefficient catalyst usage, lower reaction selectivities and, in extreme cases, to self-sustaining hot spots in the reactor. For multi-phase flow, maldistribution is an important problem because a homogeneous distribution of liquid into the monolith channels is not trivial [15,19–21]. Additionally, it was demonstrated [18] that different combinations of gas–liquid flow velocities result in the same pressure drop over a monolith, which may result in a non-homogeneous gas–liquid distribution. Residence time distribution experiments confirmed the presence of a liquid flow maldistribution, but the origin could only partially be ascribed to the distribution device [19]. For single-phase flow (usually gas flow) the distribution over the monolith channels is easier but there may be maldistribution as a result of pressure-distribution at the inlet of the monolith [22–24]. This is usually due to the shape of the inlet to the reactor.

Intrinsic maldistribution is another form of maldistribution. This type of maldistribution is induced by small variations in the geometry of the monolith channels. Consider the square channels in Fig. 1. Apart from wall-effects, the wall thickness varies from channel to channel; some channels are slightly skewed or corrugated; there may be small defects inside the channel; and some channels may become partially plugged after some time of operation. Each of these anomalies may cause intrinsic maldistribution in monoliths. Unfortunately, this effect is often neglected in literature. Maldistribution was also studied inside glass monolith channels [20] but this is an expensive and difficult experiment. This paper introduces a much more straightforward manner of determining intrinsic maldistribution for commercially available samples.

The present work focuses on gas adsorption by carbon-coated monoliths for air purification and respiratory protection [11]. Especially in respiratory protection applications the low concentration range in the effluent is of extreme importance. The concentration of a toxic compound in the breather's air must be reduced with a factor typically in the order of 20–1000 for civilian and 1000–100,000 for military users. The performance of adsorbents is expressed as a breakthrough time, which is the time at which an adsorbent bed is saturated. Maldistribution is of pivotal importance in this case because the breakthrough time is determined by the monolith channel through which the gas flow is the highest. This channel will be saturated first and will allow toxic gasses to penetrate first. Therefore, a straightforward experimental method has been developed to measure intrinsic maldistribution in monoliths. The experimental method will also be useful for other gas applications with monoliths such as automobile catalysts, and could serve as a quality control technique.

2. Background

A monolith can be seen as a bundle of parallel straight channels that are present in a single substrate. Therefore, the pressure drop over monoliths is derived from the pressure drop in these straight channels. In a gas–solid application the following derivation holds.

Consider the pressure drop over a straight channel. The single-phase pressure drop is given by [25]:

$$\frac{\Delta p}{L} = 4f\frac{(1/2)\rho_g u_g^2}{d_h} \tag{1}$$

where Δp is the pressure drop; L is the length of the channel; f is the Fanning friction factor; ρ_g is the gas density (1.24 kg/m^3); u_g is the mean gas velocity; and d_h is the hydraulic diameter of the channel. The hydraulic diameter, d_h, is defined as follows [26]:

$$d_h = \frac{4A}{P} \tag{2}$$

where A is the cross-sectional area of the flow channel and P is the wetted perimeter of the flow channel. For square channels, d_h equals the length of the side of the square. In this case d_h equals 1.09 mm for 100 cpsi monoliths and 2.11 mm for 400 cpsi monoliths.

For fully developed flow in square channels, the friction factor is [26]:

$$f = \frac{C}{Re} \tag{3}$$

where C is a constant. For round channels C equals 16. For square channels, which are relevant in this case, C equals

14.23. *Re* is the dimensionless Reynolds number:

$$Re = \frac{\rho_g u_g d_h}{\eta_g} \tag{4}$$

in which η_g is the gas viscosity (air: 1.80×10^{-5} Pa s). Eqs. (1)–(4) can be simplified to give:

$$\frac{\Delta p}{L} = 2C\frac{u_g \eta}{d_h^2} \tag{5}$$

The flow pattern close to the entrance of the channels is different from a fully developed flow pattern in the channels. This pattern is important for short monoliths. Developing flow in square channels, is incorporated as follows [25]:

$$f = \frac{C}{Re}\left(1 + 0.0445\, Re\frac{d_h}{L}\right)^{0.5} \tag{6}$$

Note that this equation holds for laminar flow conditions, which typically occurs in the small channels of the monoliths in applications for respiratory protection. It is usually assumed that the monolith channels have the same length and shape so for a certain pressure drop applied over a monolith the average velocities in all channels is the same. However, this assumption is incorrect as explained below.

Ceramic monoliths are extruded from paste and subsequently baked in an oven [27]. During the manufacturing process random variations may occur that lead to variances in the end product. Firstly, the shape of the monolith is formed by the mold of the extruder. Spatial variations in the mold introduce variances in wall thickness and channel widths of the monolith channels. Secondly, sintering is generally a nonlinear process that is difficult to control: thermal stresses may deform the channels; temperature variances may introduce varying degrees of sintering; and gases escaping the hardening paste introduce surface roughness. These processes also introduce variations in the channel widths of the monolith. Thirdly, the paste composition may vary slightly and introduce variances in channel widths.

Coating the monoliths with carbon or a washcoating introduces an additional random variation [28].

Close observation of the monolith cross-section in Fig. 1 proves that variations actually occur in real life monoliths, as may be expected from the complex production process. Especially skewed and corrugated channels are clearly present. The channels near the edge of the monolith are often not square channels. These will obviously have flow characteristics that differ from the channels in the middle of the monolith but this is not relevant to this paper. Their aerodynamic behavior will be considered as wall effects.

Accepting that channels have slightly different shapes, it is easy to see from Eq. (5) that their hydrodynamic behavior will differ. For instance, if one channel has a smaller hydraulic diameter, d_h, Eq. (5) predicts that it will have a higher pressure drop or a different flow rate, depending on the applied condition. Similarly, if the channel shape differs from a perfect square the constant *C* changes in Eq. (6).

At this point it is difficult to predict how the variations in hydrodynamic behavior should be modeled. A priori, a normal distribution is assumed unless the experimental data shows otherwise. It seems reasonable to assume that the variations in the channel dimensions are introduced as random variations in the production process. If these variations are responsible for the variations in hydrodynamic behavior, the variation in the friction factor *f* per channel may be expected to have a normal distribution.

3. Experimental setup

Pressure drop measurements were performed in individual channels of the monolith. For this purpose an experimental set-up was designed, which is shown in Fig. 2. The monoliths that were used are 100 and 400 cpsi cordierite monoliths (EX-80 by Corning, USA) with a diameter of 43 mm and a length of 250 and 52.6 mm, respectively.

Fig. 2 depicts the experimental setup, where the air flows from left to right. The air entered a single monolith channel through a perforation in the aluminum tape (type 944 ALU SE by Coroplast, Germany). Aluminum tape was used because of its strong adhesive character and because it retains its shape after it is pressed onto the monolith, it does not deform like plastic tape does. The perforation was made with a syringe needle and shaped like a single channel: square. The monolith was sealed and protected by a plastic adhesive film. Subsequently, the air left the monolith in the glass cap and flowed through the syringe needle. The syringe needle acted as a critical orifice because of the vacuum downstream. The critical orifice ensures that the flow through each individual monolith channel studied is exactly the same every time. The flow was measured with a thermal flow meter

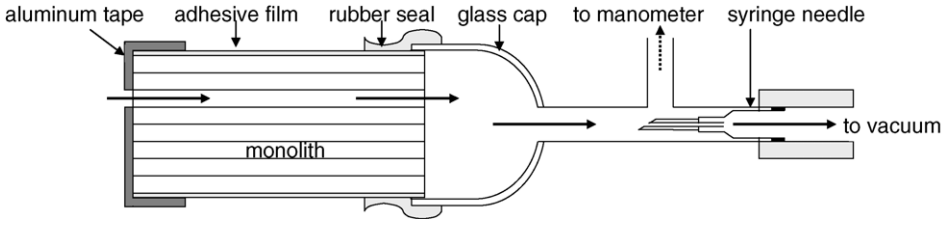

Fig. 2. Experimental setup for measuring intrinsic maldistribution in monoliths.

(4100 Series by TSI Inc., USA), which has an accuracy of 2% of reading.

The pressure drop over a single monolith channel was measured by measuring the pressure difference between the air in the glass cap and the outside air. This pressure difference was corrected with the pressure difference of the empty glass cap, which was less than 10 Pa. The pressure difference was measured with a membrane pressure transducer (type HM28 by Revue Thommen AG, Switzerland). The instrument has an accuracy of 0.1% of full scale (2500 Pa), which equals 2.5 Pa.

After the pressure drop over one channel was measured it was sealed with a small piece of aluminum tape; another channel was opened, and the pressure drop was measured again. The measurement was repeated at least 30 times. The channels were selected at random so that the measured channels were distributed uniformly over the monolith face. Channels directly near the edge of the monolith were not measured.

4. Results

The measured pressure drop data are presented in two ways, in a normal probability plot and a plot in which the probability of occurrence is shown as function of the pressure drop. The normal probability plot [29] is given because it gives much useful information about the measured data. It is constructed by plotting the (ordered) measured values versus the probability of their occurrence. In this case, the measured pressure drop for each channel is plotted on a linear y-axis and the probability of occurrence is plotted on a transformed x-axis. The transformation of the x-axis is done in such a way that if the plotted data yields a straight line, a normal distribution exists. The variable on the x-axis is given in units of variance (σ) around the mean (μ) value of a normal distribution. So the x-value 0 corresponds with the mean value of a normal distribution, +1 corresponds with +1 units of variance σ from the mean, and −2 corresponds with −2 units of variance σ from the mean. The method is used because it is easy to assess whether the data obeys a normal distribution (when the data follows a straight line); moreover, if the data obey a normal distribution it is easy to find the mean and variance of the measurements. The measured variance will be identified with s_{imc} because it is an estimator for the variance σ. Further details on the mathematical method can be found elsewhere [29].

The probability occurrence plot has an illustrative function; it shows the spread in the measured pressure drop very clearly.

Figs. 3–5 show the results. Top portion of Figs. 3–5 shows normal probability plots and bottom portion of Figs. 3–5 shows probability occurrence plots. Table 1 summarizes the relevant data.

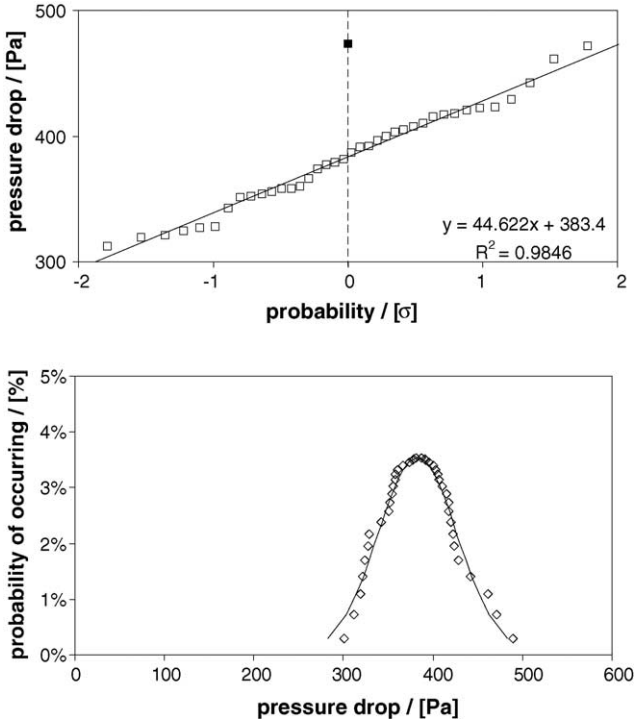

Fig. 3. Pressure drop over monolith channels at constant flow rate presented in normal probability plot (top) and a probability distribution (bottom). Conditions: channel air flow rate 1.35×10^{-5} m^3/s in a 52.6 mm long 400 cpsi cordierite monolith.

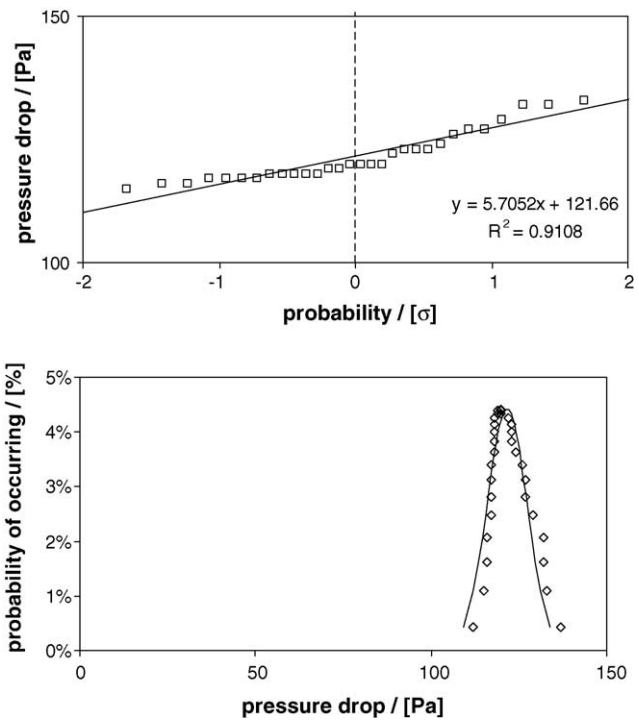

Fig. 4. Pressure drop over monolith channels at constant flow rate presented in normal probability plot (top) and a probability distribution (bottom). Conditions: channel air flow rate 1.77×10^{-5} m^3/s in a 250 mm long 100 cpsi cordierite monolith.

Table 1
Summary of pressure drop data for intrinsic maldistribution in monoliths

Data in figure	Cell density (cpsi)	Length (mm)	Channel flow rate (m^3/s)	Measured Δp (Pa)	Model Δp (Pa)
Fig. 3	400	52.6	1.35×10^{-5}	383 ± 44.6 (11.6%)	474
Fig. 4	100	250	1.77×10^{-5}	122 ± 5.71 (4.7%)	164
Fig. 5	100	250	2.81×10^{-5}	228 ± 17.6 (7.7%)	260

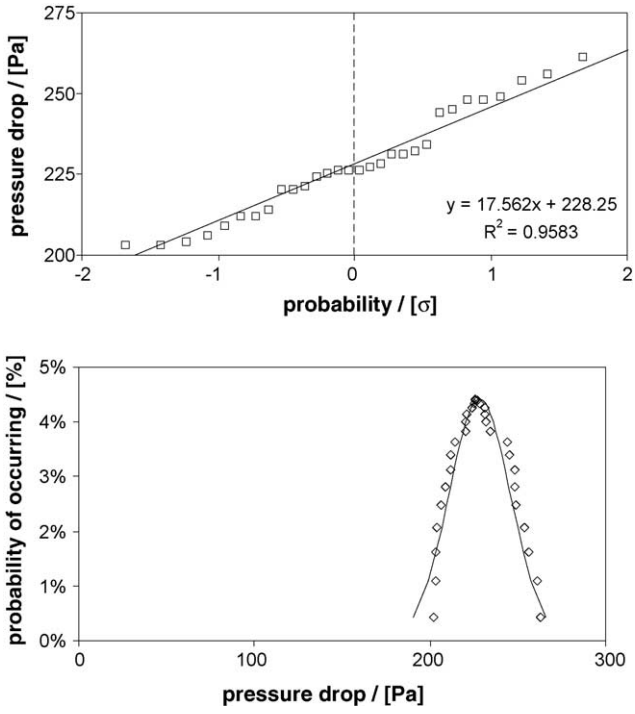

Fig. 5. Pressure drop over monolith channels at constant flow rate presented in normal probability plot (top) and a probability distribution (bottom). Conditions: channel air flow rate 2.81×10^{-5} m^3/s in a 250 mm long 100 cpsi cordierite monolith.

5. Discussion

Fig. 3 (top) shows that the data points for the 400 cpsi monolith form a straight line which implies that the pressure drop at constant flow rate through individual monolith channels can be described by a normal distribution. A straight line is fitted through the data by least squares fitting. The intercept yields the mean pressure drop of 383.4 Pa. The slope of the line equals the variance σ of 44.6 Pa or 11.6% of the mean. So, in this case, the variance in pressure drop per monolith channel can be described by a normal distribution with a measured value of 383.4 ± 44.6 Pa.

Fig. 3 (bottom) shows that the data points follow the fitted normal distribution very well: the data points exhibit a normal distribution, as could be expected from the analysis of Fig. 3 (top). This picture also illustrates that the distribution in pressure drop is quite wide. The assumption that all monolith channels can be considered to be identical is not valid.

The model that is described in Section 2 predicts a pressure drop of 473.6 Pa for a single channel (Table 1). The measured mean pressure drop of 383.4 Pa is 19% lower than the predicted value. It is possible that the model overestimates the pressure drop but it is more likely that some leakage of air through the porous walls into neighboring channels has occurred. This leakage effect does not seem to interfere much with our results since the flow resistance is of the walls is very high and the deviation from the predicted value is relatively small.

Similar considerations hold for the experiments with a 100 cpsi monolith as the results in Table 1 show. However, the variance in the measured data is smaller: 4.7% and 7.7%. The variances in the production process have less influence on the intrinsic maldistribution of these monolith channels. This is logical because the channels are wider and the monolith walls are thicker and thus it is easier to extrude monoliths that are stronger and less prone to spatial deformations of individual monolith channels. Also here the observed pressure drop is 15–30% lower than predicted. Again, it is possible that the model overestimates the pressure drop but it is more likely that leakage into neighboring channels has occurred.

The variance in measured pressure drop may be caused by many different factors. They are briefly discussed here.

Variances in the hydrodynamic diameter d_h of the channels and in the friction factor f through the constant C have a large influence on pressure drop over a single monolith channel. In theory the monolith length L may also vary but a square cut should prevent this. The theoretical background illustrates that if the channel shape is not square, the constant C changes. If the channels differ slightly in size or shape, d_h changes. In turn, the friction factor f is not a constant but variances in surface roughness also influence the friction factor. In addition, these parameters may alter entrance effects inside the channel so the constant 0.0455 in Eq. (5) may be different. “Entrance” effects may occur upstream of the monolith as well, i.e. if a large channel draws a lot of gas, the gas flow in a small neighboring channel may be influenced.

From a phenomenological standpoint it is interesting to know which of the parameters above contributes the most. Unfortunately, the effects of these factors are lumped into the overall variances that are measured as a normal which makes it very difficult to estimate which of these factors is more important than the other. From a practical standpoint, however, it suffices to know that their combined effect is lumped in a normal distribution, which has to be incorporated when mathematical models are developed for monolithic reactors.

The pressure drop is reported per channel as function of a fixed flow rate. In practice, however, there will be a fixed pressure drop over the monolith and the flow rate in the channel varies. This is no limitation for applying this experimental method to study intrinsic maldistribution, because the flow through the individual monolith channels is laminar: the Reynolds numbers are calculated to be 1103, 734, and 1168 for experiments 1–3, respectively. These *Re*-numbers are below 2000, so indeed in the laminar regime. In the laminar flow regime, the pressure drop Δp and the gas velocity u_g are proportional. Thus, a variance in the pressure drop is directly linked to a variance in the gas velocity. Therefore, the variance in pressure drop at a fixed flow, as measured here, is similar to the variance in flow velocity when the pressure drop over the monolith is fixed. In turn, the variance in velocity is a measure for the variance in average residence times of gases in the monolith channels, which is important for modeling catalytic or adsorption processes inside the monolith. Therefore, it is recommended to include a normal velocity distribution in modeling monoliths as gas–solid reactors. The experimental method described here can provide the necessary velocity distribution.

Incorporating the observed distribution in the hydrodynamic correlations one may use a distribution in the effective hydrodynamic diameter d_h, being the square root of the velocity distribution (see Eq. (5)). For developed laminar flow this choice is similar as using the constant *C*, but for developing flow these choices can yield a different result, due to the presence of the *Re* number in the term expressing the excess friction due to the flow development, see Eq. (6).

6. Experimental indications

The results in this paper are based on a single-phase gas–solid system so it is interesting to predict what impact it will have on residence time distributions of gas, liquid and gas–liquid applications of monoliths. The impact is illustrated with some calculations of the residence time distribution in a bundle of (round) channels. Only key mathematical equations are reported here. Further details can be found elsewhere [30].

The effect of (neglecting) the velocity distribution on monoliths in adsorption applications has been demonstrated elsewhere [11].

Consider a gas that is dissolved in a fluid which flows through a (round) single tube under laminar flow conditions. There are three principal regimes can be distinguished for the residence time distribution of the gas [30]. The first is the pure diffusion regime where the fluid flow velocity is negligible when compared to the average diffusion velocity of the dissolved gas. The second is the pure convection regime where the diffusion velocity of the gas is negligible to the average fluid flow velocity. The third is the dispersion regime where the velocities are comparable. Here, we discard the pure diffusion regime because it is not applicable to filtration applications of monoliths.

The residence time distribution of the pure convection model can be captured by the following equation [30]:

$$E(\Theta) = \frac{1}{2\Theta^3} \quad \text{for } \Theta \geq \frac{1}{2} \tag{7}$$

where Θ is the arithmetic residence time: the volume of the tube divided by the volumetric fluid flux in the tube. The residence time distribution for the dispersion regime can be captured by:

$$E(\Theta) = \frac{1}{\sqrt{4\pi(D_{ax}/u_g L)}} \exp\left[-\frac{(1-\Theta)^2}{4(D_{ax}/u_g L)}\right] \tag{8}$$

where D_{ax} axial dispersion coefficient of the dissolved gas in the carrier fluid. Actually, Eq. (8) does not cover the whole dispersion regime but only in cases where the dissolved gas behaves as in a plug flow reactor.

Experiment 2 is used as the blueprint for calculations of the residence time of a pollutant in a monolithic filter at ambient conditions. Differences are: the monolith reactor length is 5 m and the pollutant is assumed to be non-adsorbing. The carrier fluids are air and water, and the pollutant is toluene that has a diffusion coefficient of 7.9×10^{-6} m^2/s in air (D_a) and 8.6×10^{-10} m^2/s in water (D_w). The air flux is 1.77×10^{-5} m^3/s for which the Reynolds number is 734. The water flux is corrected to have the same Reynolds number as with air.

Theory suggests that the calculation for the residence time of toluene in air is governed by Eq. (8) [30]. In this specific case, the axial dispersion coefficient is:

$$D_{ax} = \frac{u_g^2 d_h^2}{192 D_a} \tag{9}$$

The residence time distribution for toluene in water is governed by Eq. (7). The calculated residence time distributions for single channel flow are shown in Fig. 6.

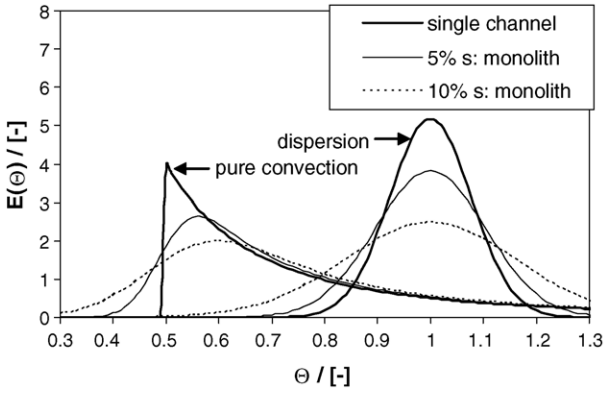

Fig. 6. The broadening effect on residence time distribution in monoliths: toluene in water (pure convection) toluene in air (dispersion model). Calculations performed in 5 m 100 cpsi monolith.

Now consider a system of multiple single tubes. This paper shows that intrinsic channel maldistribution adds to the broadening of the residence time distribution. So, we can superimpose the variance created by intrinsic maldistribution over the residence time distribution of a single channel. For air, in this case, the variance of maldistribution is added in a straightforward manner in the axial dispersion coefficient:

$$D_{ax} = \frac{u_g^2 d_h^2}{192 D_a} + s_{imc}^2 \quad (10)$$

where s_{imc} is the measured variance that is introduced by the intrinsic channel maldistribution. For water, the variance of maldistribution is introduced by calculating a weighed normal distribution with a variance of s_{imc} on each point on the $E(\Theta)$ for water. The results are summed and normalized to give the new $E(\Theta)$ curve. Fig. 6 shows the results for a maldistribution variance (s_{imc}) of 5% and 10% which is in the range that our measurements indicate.

The results in Fig. 6 clearly show that intrinsic cannel maldistribution broadens the residence time distribution quite much with only a 5% variance. The sharp peak in the pure convection model disappears and a plug flow like curve appears. Thus, by measuring the residence time distribution in a monolith, pure convection would never be found.

Monoliths are also used in gas–liquid systems. In practical applications the flow occurs as a so-called Taylor or bubble train flow where liquid plugs are separated by a train of water bubbles. The friction factor for this three phase flow pattern is [19]:

$$f = \frac{16}{Re}\left[1 + 0.17\frac{1}{\Psi_s}\left(\frac{Re}{Ca}\right)^{0.33}\right] \quad (11)$$

The mathematical description is similar to that of developing single-phase flow [19]. It includes the dimensionless slug length Ψ_s and the capillary number Ca, accounting for the presence of the gas–liquid interfaces. This contribution may increase the friction up to four times that for single-phase flow. Term 0.17 is a correction factor that describes interfacial effects of Taylor bubbles in the channel (Laplace pressure term), which is fairly constant. So, even in Taylor flow, the pressure drop is dominated by viscous friction with the walls. As a result, it is expected that the intrinsic channel distribution has a similar effect on the residence time distribution as for single phase flow.

The residence time distribution is governed by the dispersion model if the flow in the monolith channels is turbulent. The impact of intrinsic channel distribution on turbulent flow is expected to be similar as sketched in Fig. 6.

7. Conclusions

The paper introduces a straightforward method to measure intrinsic maldistribution in monoliths in gas–solid operation. The experimental procedure can be easily applied to commercial samples, is non-destructive for the monolith, but special care has to be taken to prevent leakage.

Intrinsic channel maldistribution can introduce substantial differences in the residence time of a substance in the monolith. As a consequence, the assumption that a monolith is a bundle of *identical* channels is incorrect and may introduce significant errors in mathematical models for monolithic reactors or adsorption columns that do not incorporate this effect. In reality, a monolith is a bundle of *slightly differing* channels. The small differences have an influence on the residence time distribution that can be described by a normal distribution. The measurements in this paper show measured variances (s_{imc}) between 11.6% and 4.7%.

It is concluded that the production process of ceramic monoliths leads to variances in channel dimensions and surface roughness. These variances lead to variances in pressure drop in a single monolith channel if the flow through the channels is equal. The mathematical models of Section 2 show that it is easy to understand this phenomenon. Small variances in the structure of the monolith influence the hydraulic diameter and the constant C in the equations so that the pressure drop is influenced. During operation, other contributions can add variations: soiling and attrition.

References

[1] R.M. Heck, R.J. Farrauto, Catalytic Air Pollution Control: Commercial Technology, Van Nostrand Reinhold, New York, 1995.
[2] R.M. Heck, S. Gulati, R.J. Farrauto, The application of monoliths for gas phase reactions, Chem. Eng. J. 82 (2001) 149–156.
[3] J.L. Williams, Monolith structures, materials, properties and uses, Catal. Today 69 (2001) 3–9.
[4] A. Cybulski, J.A. Moulijn, Monoliths in heterogeneous catalysis, Cat. Rev. Sci. Eng. 36 (1994) 179–270.
[5] T. Valdés-Solís, G. Marbán, A.B. Fuertes, Low-temperature SCR of NO_x with NH_3 over carbon-ceramic supported catalysts, Appl. Catal. B: Environ. 46 (2003) 261–271.
[6] T. Valdés-Solís, G. Marbán, A.B. Fuertes, Low-temperature SCR of NO_x with NH_3 over carbon–ceramic cellular monolith-supported manganese oxides, Catal. Today 69 (2001) 259–264.
[7] M.A. Buzanowski, R.T. Yang, Simple design of monolith reactor for selective catalytic reduction of NO for power plant emission control, Ind. Eng. Chem. Res. 29 (1990) 2074–2078.
[8] J. Blanco, P. Avila, S. Suarez, J.A. Martin, C. Knapp, Alumina- and titania-based monolithic catalysts for low temperature SCR of NO, Appl. Catal. B: Environ. 28 (2000) 235–244.
[9] K.P. Gadkaree, Carbon honeycomb structures for adsorption applications, Carbon 36 (1998) 981–989.
[10] M. Yates, J. Blanco, P. Avila, M.P. Martin, Honeycomb monoliths of activated carbons for effluent gas purification, Micropor. Mesopor. Mater. 37 (2000) 201–208.
[11] T. Valdés-Solís, M.J.G. Linders, F. Kapteijn, G. Marbán, A.B. Fuertes, Adsorption and breakthrough performance of carbon-coated ceramic monoliths at low-concentration *n*-butane, Chem. Eng. Sci. 59 (13) (2004) 2791–2800.
[12] F. Kapteijn, J.J. Heiszwolf, T.A. Nijhuis, J.A. Moulijn, Monoliths in multiphase catalytic processes—aspects and prospects, CATTECH 3 (1999) 24–41.
[13] R. Edvinsson Albers, M. Nystrom, M. Siverstrom, A. Sellin, A.C. Dellve, U. Andersson, W. Herrmann, T. Berglin, Development of a

monolith-based process for H_2O_2 production: from idea to large-scale implementation, Catal. Today 69 (2001) 247–252.
[14] J.H.B.H. Hoebink, G.B. Marin, Modeling of monolithic reactors for automotive exhaust gas treatment, in: A. Cybulski, J.A. Moulijn (Eds.), Structured Catalysts and Reactors, Marcel Dekker Inc., New York, 1998, pp. 209–237.
[15] A.K. Heibel, T.W.J. Scheenen, J.J. Heiszwolf, H. Van As, F. Kapteijn, J.A. Moulijn, Gas and liquid phase distribution and their effect on reactor performance in the monolith film flow reactor, Chem. Eng. Sci. 56 (2001) 5935–5944.
[16] P. Woehl, R.L. Cerro, Pressure drop in monolithic reactors, Catal. Today 69 (2001) 171–174.
[17] J.J. Heiszwolf, L.B. Engelvaart, M.G. Van den Eijnden, M.T. Kreutzer, F. Kapteijn, J.A. Moulijn, Hydrodynamic aspects of the monolith loop reactor, Chem. Eng. Sci. 56 (2001) 805–812.
[18] M.T. Kreutzer, F. Kapteijn, J.A. Moulijn, C. Kleijn, J.A. Heiszwolf. Pressure drop of Taylor flow in capillaries, AIChE J., in press.
[19] M.T. Kreutzer, J.J.W. Bakker, F. Kapteijn, J.A. Moulijn, P.J.T. Verheijen. Scaling-up multiphase monolith reactors: linking residence time distribution and flow maldistribution, Ind. Eng. Chem. Res., in press.
[20] I.V. Koptyug, S.A. Altobelli, E. Fukushima, A.V. Matveev, R.Z. Sagdeev, Thermally Polarized 1H NMR microimaging studies of liquid and gas flow in monolithic catalysts, J. Magn. Reson. 147 (2000) 36–42.
[21] Z. Olujić, A. Mohamed Ali, P.J. Jansens, Effect of the initial gas maldistribution on the pressure drop of structured packings, Chem. Eng. Process. 34 (2004) 465–476.
[22] J. Wollin, S.F. Benjamin, A study of the flow performance of ceramic contoured substrates for automotive exhaust catalyst systems, SAE Technical Paper Series 1999-01-3626, 1999.
[23] A.P. Martin, A.E. Massey, M.V. Twigg, N.S. Will, J.M. Davidson, A chemical method for the visualisation of flow maldistribution in a catalytic converter, SAE Technical Paper Series 1999-01-3076E, 1999.
[24] A. Holmgren, T. Gronstedt, B. Andersson, Improved flow distribution in automotive monolithic converters, React. Kinet. Catal. Lett. 60 (1997) 363–371.
[25] R.B. Bird, W.E. Stewart, E.N. Lightfoot, Transport Phenomena, John Wiley & Sons, New York, 1960.
[26] F.M. White, Fluid Mechanics, McGraw-Hill, New York, 1999.
[27] X. Xu, J.A. Moulijn, Transformation of a structured carrier into a structured catalyst, in: A. Cybulski, J.A. Moulijn (Eds.), Structured Catalysts and Reactors, Marcel Dekker Inc., New York, 1998, pp. 599–616.
[28] T.A. Nijhuis, A.E.W. Beers, Th. Vergunst, I. Hoek, F. Kapteijn, J.A. Moulijn, Preparation of monolithic catalysts, Catal. Rev. Sci. Eng. 43 (4) (2001) 345–380.
[29] J.L. Devore, Probability and Statistics for Engineering and the Sciences, Duxbury, Pacific Grove, 1999.
[30] O. Levenspiel, Chemical Reactor Engineering, John Wiley & Sons, New York, 1999.